SCIENTIFIC REPORTS
nature research

OPEN

The Influence of Oil leaking rate and Ocean Current Velocity on the Migration and Diffusion of Underwater Oil Spill

Hong Ji[1,2], Manlin Xu[1,2], Weiqiu Huang[1,2] ✉ & Ke Yang[3] ✉

Severe environmental pollution and huge economic losses would be caused by submarine oil spill with the increasing development of petroleum energy in sea. In order to predict the law of migration of oil spill from submarine pipelines accurately, the volume of fluid (VOF) model and realizable *k-ε* turbulence model were employed to establish numerical simulation of submarine oil spill, and the experiments were used to verify the feasibility of the numerical models. Different oil leaking rate and ocean velocity were simulated in the study. The simulation results indicated that comparing with oil leaking rate (set vertical migration velocity, U_o), current velocity (set horizontal migration velocity, U_w) has a greater influence on the migration of the oil spilling; the actual vertical migration velocity (U_{o1}), actual horizontal migration velocity (U_{w1}) and R_1 (the ratio of U_{o1} and U_{w1}) are positively correlated with R (the ratio of U_o and U_w), and they both fluctuate within a small range no matter how large R is; when $20 \leq R \leq 150$, R_1 fits a linear fit curve with curve as $R_1 = 0.66932 + 0.00215R$, which can provide a theoretical reference to the recovery system of underwater pipeline oil spilling emergency.

With the gradual depletion of land resources, people have turned their eyes to the ocean. Submarine pipelines are the lifelines of offshore oil and gas fields. However, submarine pipelines are in a harsh environment for a long time and normally damaged under various unforeseen risks[1], which could cause oil spills[2]. In the event of oil spill, it will cause huge economic losses and lead to a series of adverse social effects. Therefore, accurate prediction of the diffusion pattern and behavior of oil spills is important to the risk assessment of oil spills, emergency response and control of the pollutants.

In recent decades, more than 50 models have been developed to predict the behavior and process of oil spills[3–5]. Hirst[6] numerically investigated 2D and 3D models of buoyant jets of oil spill, and verified correctness of them by comparing them with the experimental results under currents. Mcdougall[7], Milgram[8] and Fanneløp, *et al.*[9] established well oil spill models without considering the action of currents. Bemporad[10] simulated the buoyant jet trajectories of a circular hole in stratified flow. Yapa *et al.*[4] established an underwater oil spill model for shallow water environments. Johansen[11], Yapa and Zheng[4,12] established the deep sea oil spill models DeepBlow and CDOG respectively, which both have been well applied in the emergency treatment and prediction process of submarine oil spill accidents. And after that, these two models were revised and improved by other scholars, and the underwater oil spill was simulated and predicted successfully[13–15]. Ben-Mansour *et al.*[16] established a 3D turbulence model to simulate small-diameter underwater leakage under realistic velocities and pressures, which showed significant features in the pressure and pressure gradient variations along the pipeline. Reed *et al.*[17] established a POSCOEM model including the Release Module and the Near Field Module to estimate the leakage of the submarine pipeline. Certain scholars in China have also begun to study the numerical simulation of underwater oil spills actively. Wang *et al.*[5] simulated the oil spill and sea surface drift of submarine pipelines based on POM and FVCOM hydrodynamic models. Liao *et al.*[18] established an oil spill model to investigate the dynamic behavior of oil and gas under different working conditions based on the Lagrangian integral method. Chen *et al.*[19] simulated the underwater oil spill trajectory based on Lagrangian integral method and particle tracking method.

[1]Jiangsu Key Laboratory of Oil & Gas Storage and Transportation Technology, Changzhou University, Changzhou, 213016, Jiangsu, China. [2]School of Petroleum Engineering, Changzhou University, Changzhou, 213016, Jiangsu, China. [3]School of Environment and Safety Engineering, Changzhou University, Changzhou, 213164, Jiangsu, China. ✉e-mail: hwq213@cczu.edu.cn; yangke728@163.com

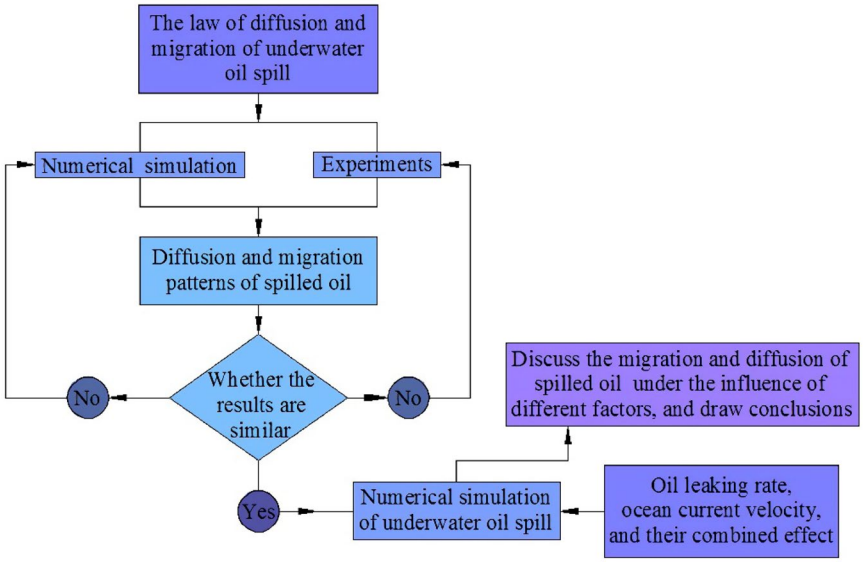

Figure 1. Research method and steps.

Lu *et al.*[20] used the VOF model to perform the leakage trajectory and diffusion of oil under effects of different factors. Li *et al.*[21] analyzed the oil and gas leakage process at different leakage locations of underwater separators of ultra-deep water. Li *et al.*[22] established a 3D drift prediction model for semi-submersible oil and sinking oil, and developed a GIS-based Bohai sea semi-submersible bottom oil risk management information system, which realized the functions of oil drift prediction and backflow calculation of oil spill trajectory.

There are many factors affecting the spread and migration trajectory of spilled oil, including oil leaking rate, ocean current velocity, oil density, leak diameter, ambient temperature and water depth, etc. Lu *et al.*[23] determined the influence of different factors on the submarine oil spill based on sensitivity analysis of the influencing factors. Zhu *et al.*[24–26] investigated the underwater spread and surface drift of oil spilled from a submarine pipeline under the combined action of wave and current. Yang *et al.*[27] established an underwater oil spill model, and verified the correctness of the model through experiments. The factors such as oil leaking rate, leak diameter, ocean current velocity and oil density were studied the impact of the migration pattern. Furthermore, some researches refer to a vertical jet introduced into a free-surface water tank in a current environment[28–31].

When the spilled oil migrates to the free surface, it would drift away or evaporate into the atmosphere under the influence of various factors, such as wind, waves, oil area and oil thickness. As a significant factor, the oil thickness has a very close relationship with the drift range and evaporation rate of spilled oil on the free surface, which mainly depends on the density and viscosity of spilled oil. The MODIS satellite visual-spectrum broadband data[32], and synergic use of optical remote-sensing and numerical modelling can both detect and characterize marine oil slicks[33]. And the later method has also been proved correct in Literature[34].

According to previous studies, the oil leaking rate and ocean current velocity are respectively two factors that have a greater impact on migration pattern of submarine oil spill. Most of the existing investigations are carried out on the influence of various single factors on migration and diffusion of underwater oil spill, and there is a lack of investigation of influence of multiple factors on it. Moreover, most of the literatures have investigated the correlation between factors and migration velocity (positive or negative), and there is a lack of experimental or numerical data did not do more quantitative analysis between factors and oil migration and diffusion parameters. Therefore, the migration pattern of submarine oil spill under the combined action of oil leaking rate and current velocity will be discussed in this study. The research methods and steps of this paper are shown in Fig. 1.

Mathematical model and numerical approach

Governing equations. The underwater diffusion process and surface drifting of oil spill both follows three laws of mass conservation, momentum conservation and energy conservation. Oil and water are set as incompressible fluids. The turbulence equation uses the realizable k-ε model, and the VOF model is used to obtain the volume fraction equation and the momentum equation. Conservation equations are as follows:

The RANS (Rey-nolds-Averaged-Navier-Stokes) equations are used to describe liquid flow, which including continuity equations and momentum conservation equations as follows[35]:

$$\frac{\partial u_i}{\partial x_i} = 0 \tag{1}$$

$$\frac{\partial u_i}{\partial t} + \frac{\partial u_i u_j}{\partial x_j} = -\frac{\partial \overline{p}}{\rho \partial x_i} + \upsilon \nabla^2 u_i - \frac{\partial x'_i x'_j}{\partial x_j} + g_i \tag{2}$$

where: u_i and u_j indicate instantaneous velocity components in i and j directions, respectively; x_i indicates the spatial coordinate in i direction; g_i is the gravitational acceleration in i direction; t indicates the time; p indicates the pressure; ρ and v represent the density and kinematic viscosity, respectively.

The VOF method is a solution to the fluid volume fraction equation based on a mixed phase momentum equation[36,37]. In this study, F_w and F_o are used to represent the fluid volume fraction in the water region and the oil region, respectively. The physical meaning of the F function is the fraction of the liquid phase volume of a unit. The liquid volume functions F_w and F_o are written as follows:

$$F_w = \frac{V_w}{V_c} \tag{3}$$

$$F_o = \frac{V_o}{V_c} \tag{4}$$

Where: F_w and F_o are volumetric functions of water and oil, respectively; V_c, V_w and V_o are the volume of one unit volume, one unit of water and oil, respectively. And the subscript w and o indicate water and oil, respectively.

Fractional function of two-dimensional transport equations:

$$\frac{\partial F_w}{\partial t} + \frac{\partial u F_w}{\partial x} + \frac{\partial v F_w}{\partial y} = 0 \tag{5}$$

$$\frac{\partial F_o}{\partial t} + \frac{\partial u F_o}{\partial x} + \frac{\partial v F_o}{\partial y} = 0 \tag{6}$$

The density and kinematic viscosity are written as follows:

$$\rho = (1 - F_o)\rho_w + F_o\rho_o \tag{7}$$

$$v = (1 - F_o)v_w + F_o v_o \tag{8}$$

Realizable k-ε turbulence model[38–40] including two equations for turbulent kinetic energy and turbulent kinetic energy dissipation rate is written as:

$$\rho\frac{\partial k}{\partial t} + \rho u_i\frac{\partial k}{\partial x_i} = \frac{\partial}{\partial x_j}\left[\left(\mu + \frac{\mu_t}{\sigma_k}\right)\frac{\partial k}{\partial x_j}\right] + G_{\mathrm{k}} + G_b - \rho\varepsilon \tag{9}$$

$$\rho\frac{\partial \varepsilon}{\partial t} + \rho u_i\frac{\partial \varepsilon}{\partial x_i} = \frac{\partial}{\partial x_j}\left[\left(\mu + \frac{\mu_t}{\sigma_\varepsilon}\right)\frac{\partial \varepsilon}{\partial x_j}\right] + \rho C_1 S\varepsilon - \rho C_2\frac{\varepsilon^2}{k + \sqrt{v\varepsilon}} + C_1\varepsilon(1 - C_\varepsilon)\frac{\varepsilon}{\mathrm{k}}G_{\mathrm{b}} \tag{10}$$

where: $\mu_t = \rho C_\mu\frac{k^2}{\varepsilon}$, $G_k = -\rho u'_i u'_j\frac{\partial u_j}{\partial x_j}$, $G_b = -g\frac{\mu_t}{\mathrm{Pr}_t}\frac{\partial \rho}{\rho \partial x_i}$, $C_1 = \max\left(0.43, \frac{\eta}{\eta+5}\right)$, $\eta = S\frac{k}{\varepsilon}$, $S = \sqrt{2S_{ij}\cdot S_{ij}}$ n, $S_{ij} = \frac{1}{2}\left(\frac{\partial u_i}{\partial x_j} + \frac{\partial u_j}{\partial x_i}\right)$, $C_1 = 1.44$, $C_2 = 1.92$, $C_\varepsilon = 1$, $C_\mu = 0.09$, $Pr_t = 0.85$, $\sigma_k = 1$, $\sigma_\varepsilon = 1.2$

In these equations: G_k and G_b represent the turbulent energy k caused by the average velocity gradient and buoyancy, respectively; k and ε indicate the amount of enthalpy per unit mass and the rate of turbulent flow energy dissipation, respectively; σ_k and σ_ε are turbulent prandtl numbers; μ and μ_t indicate the dynamic viscosity and turbulent viscosity, respectively.

Computational domain and boundary conditions. A 2D flow model with a leak of 0.02 m in diameter was employed, and the whole computational domain was a rectangle with a length of 10 m and a height of 4 m. The coordinate origin was located at the lower left corner of the domain. In terms of numerical simulation, the densities of water and oil were set as 998 kg·m^{-3} and 730 kg·m^{-3}, respectively. The viscosities of water and oil were set as 1.003×10^{-3} Pa·s and 2.4×10^{-3} Pa·s, respectively. As shown in Table 1, the oil leaking rate (U_o) and ocean current velocity (U_w) were varied from case to case.

In order to obtain a higher-quality simulation model, and obtain the simulation results more efficiently, the sensitivity analysis was performed on the four models with different grid numbers (36000, 56000, 81000 and 144000). In the numerical simulation of underwater oil spill, the time for the oil to migrate to the surface and the horizontal migration distance are of great significance for emergency response to underwater oil spills. Therefore, when verifying the grid sensitivity in this paper, the oil floating time to the water surface and the change of the horizontal migration distance when the migration time is 10 s under the four grid quantity models are investigated. The results are shown in Fig. 2. It can be seen that the migration time and horizontal migration distance obtained under the four grid numbers were relatively close, and the continued increase in the number of grids has little effect on the calculation results. Moreover, the calculation time of the model is positively correlated with the number of grids. In consideration of safety and calculation time, the model with the largest horizontal migration distance was selected.

Case	Oil leaking rate/U_o (m·s^{-1})	Ocean current velocity/U_w (m·s^{-1})	$R = U_o/U_w$
1	4	0.1	40
2	10	0.1	100
3	15	0.1	150
4	4	0.2	20
5	10	0.2	50
6	15	0.2	75
7	10	0.5	20
8	10	1	10
9	12	0.1	120
10	12	0.5	24
11	12	1	12
12	4	0.8	5
13	10	2	5
14	6	0.3	20
15	3	0.1	30
16	6	0.2	30
17	9	0.3	30
18	8	0.2	40
19	12	0.3	40

Table 1. Simulation cases.

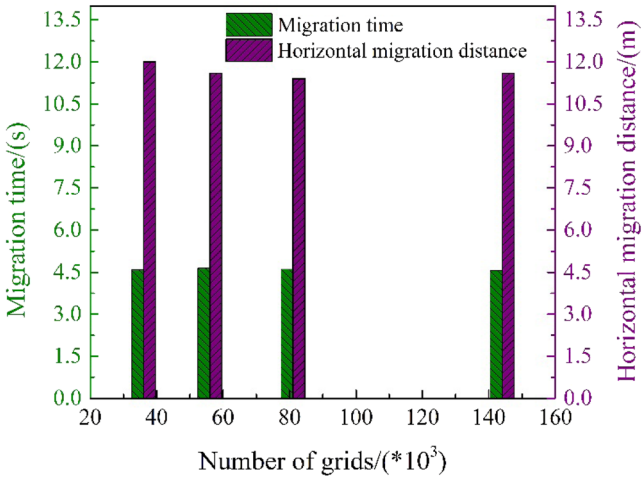

Figure 2. Comparison of simulation results under different numbers of grids.

Simulation and experimental verification. In order to ensure the accuracy of the simulation results, experiments were carried out to judge whether the simulation model and method were feasible. The parameters of the simulation model was the same as the parameters of the experiment. In terms of the experiment and numerical simulation, the water depth was 0.4 m, the width of the water tank was 2.4 m, and the diameter of leak hole was 1.5 mm. The densities of water and oil were 998 kg·m^{-3} and 915 kg·m^{-3}, respectively. The flow rate of pipeline was 44 L·min^{-1} and the oil leaking rate was 1.494 m·s^{-1}. Pressure sensors and high-speed camera were applied to collect experimental data. The heights of pressure measuring points for 1 to 3 on Y axis were set at 10, 20 and 30 mm above the leak hole (Fig. 3).

Figure 4 presents the migration and diffusion of underwater oil at the process of the experiments. Figure 5 shows the comparison between the experimental values (EVs) and simulation values (SVs) of pressure and vertical migration distance, respectively. The SVs were generally consistent with EVs except a slight deviation between them. The error between SV and EV of the average value of the pressure at each measuring point was between 4.5% and 6.7%, and the error between SV and EV of the vertical migration velocity was 2.3%. It could be concluded that the simulation method was reasonably employed to investigate the law of diffusion and migration of submarine oil spill.

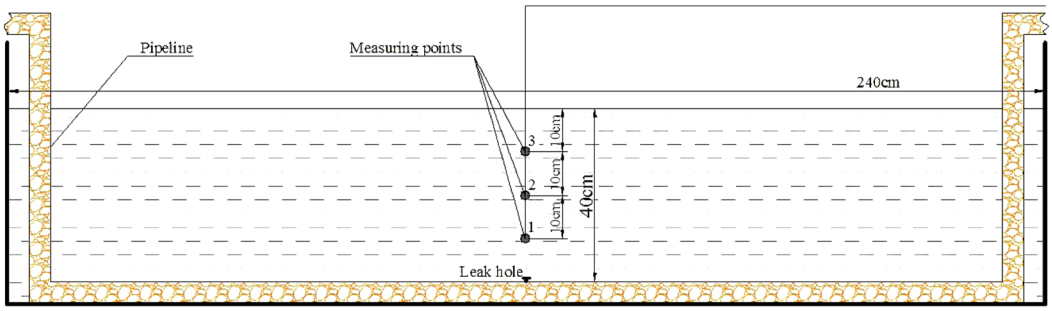

Figure 3. The location of the pressure measuring points.

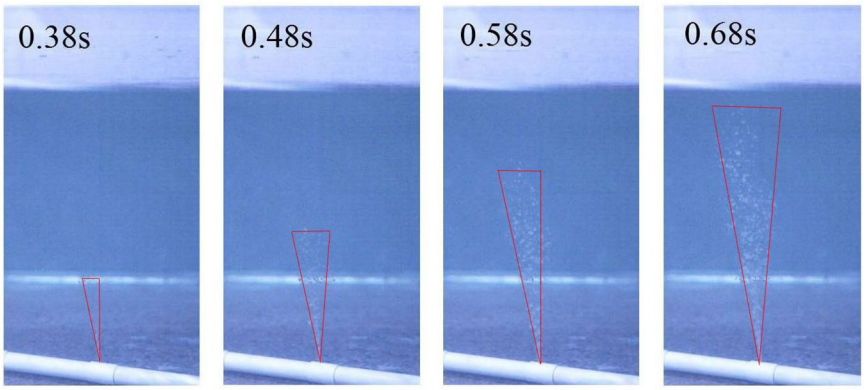

Figure 4. The migration and diffusion of underwater oil at the process of the experiments.

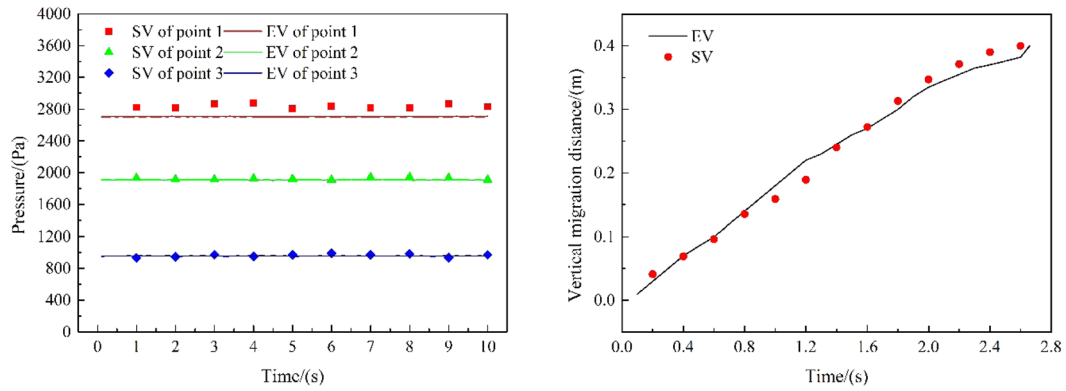

Figure 5. Comparison between EVs and SVs of pressure of measuring points **(a)** and vertical migration distance **(b)**.

Results and discussions

Effect of oil leaking rate (U_o). When studying the effects of different factors on submarine oil spills, many scholars have found that the larger the oil leaking rate, the larger the initial momentum is and the shorter the time to reach the water surface[40–43]. Numerical simulation were carried out under two groups of simulation cases (Case 1 to Case 3 as a group and Case 4 to Case 6 as a group). These two groups of cases were selected to discuss the effect of different U_o on underwater oil spill. The floating processes of oil spilling from the leak under different oil leaking rate (U_o) when the current velocities are 0.1 and 0.2 $m \cdot s^{-1}$ are shown in Figs. 6 and 7, respectively. We assumed that the vertical migration velocity of spilled oil only under their buoyancy is the same.

Some scholars have divided the process of underwater oil spill into three stages[27,44,45]: buoyancy jet stage, buoyancy plume stage and advection diffusion stage. However, the process are divided into two stages[4,12,46] by some other scholars: plume jet stage and buoyancy diffusion stage. The spilled vertical oil stream releases from the leak with the initial momentum, which forms the first entrainment vortexes on both sides of jet at the plume jet

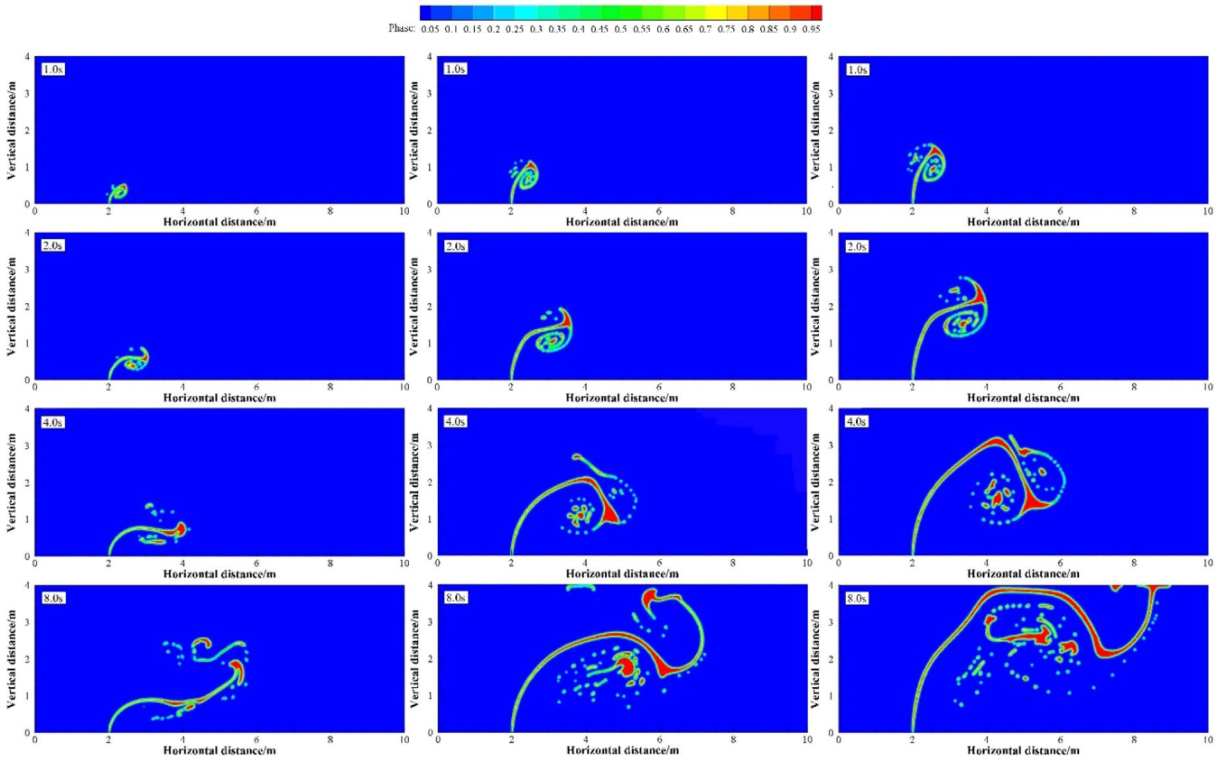

(a) Case 4 (b) Case 5 (c) Case 6

Figure 6. The migration and diffusion of underwater oil at different oil leaking rates when $U_w = 0.1\ m \cdot s^{-1}$.

stage. After the initial momentum is exhausted, the dispersed oil droplets mainly migrates with the motion trail of buoyancy and ocean currents, which is the buoyancy diffusion stage.

It can be seen from Figs. 8 and 9 that the larger U_o is, the larger the first entrainment vortexes are. The entrainment vortex on the left side of jet is dispersed into oil droplets of different sizes with the motion of ocean currents. However, the entrainment vortex on the right side becomes gradually larger. Then the second entrainment vortex is formed on both sides of the jet, which slows down the migration velocity of the jet. The dispersed oil droplets are accumulated at the lower right side of the jet. The larger U_o is, the more oil droplets accumulated. In this process, more and more dispersed oil droplets are separated under the control of the entrainment vortex, and move up slowly with the motion of buoyancy and ocean currents.

The larger U_o is, the less the initial migration pattern of oil leakage is affected by the ocean current, and the greater the change in the vertical migration velocity of the jet is. In the first stage of jet, the spilled oil in all cases migrates to the surface with different initial oil leaking rate, and the jet is less affected by the ocean current because of the initial momentum. However, in the second stage, the jet gradually loses control of the initial momentum. Spilled oil migrates along the direction of the ocean current under the influence of ocean current and buoyancy, and the jet trajectory is greatly deviated. The vertical migration velocities of jet are reduced to a same value only under the influence of buoyancy (Fig. 8). When U_o is smaller, the vertical velocity difference between two stages of jet is smaller because of the smaller initial momentum, so the vertical migration curve is smoother. It can also be seen from Fig. 9 that both the average horizontal migration velocities (U_{w1}) and average vertical migration velocities (U_{o1}) are linearly and positively correlated with U_o. As shown in Fig. 10, we defined the migration height and migration width as the vertical migration length (L_o) and horizontal migration length (L_w) of spilled oil, respectively. And the ratio of L_o to migration time (t_o) was U_{o1}, and the ratio of L_w to t_o was U_{w1}.

Effect of ocean current velocity (U_w). Numerical simulations were carried out under two groups of simulation cases (Case 2, 7 and 8 as a group; Case 9 to 11 as a group). These two groups of cases were selected to discuss the effects of different U_w on underwater oil spill. The floating processes of oil spilling motion from the leak under different U_w when the oil leaking rates were 10 and $12\ m \cdot s^{-1}$ are shown in Figs. 11 and 12, respectively.

It can be seen from the following figures that ocean current velocity also has a great influence on the migration of spilled oil. Firstly, when oil leaking rate is $10\ m \cdot s^{-1}$ (Fig. 11), the larger U_w is, the smaller the entrainment vortex on the left side during the first entrainment movement. When $U_w = 1\ m \cdot s^{-1}$, the first entrainment vortex only exists on the right side. Secondly, the larger the ocean current velocity is, the more oil droplets accumulates under the control of the entrainment motion and the initial momentum; and the lower the height of the oil droplets accumulation is, the more slowly the spilled oil migrates to the surface. Finally, according to the figures, the larger

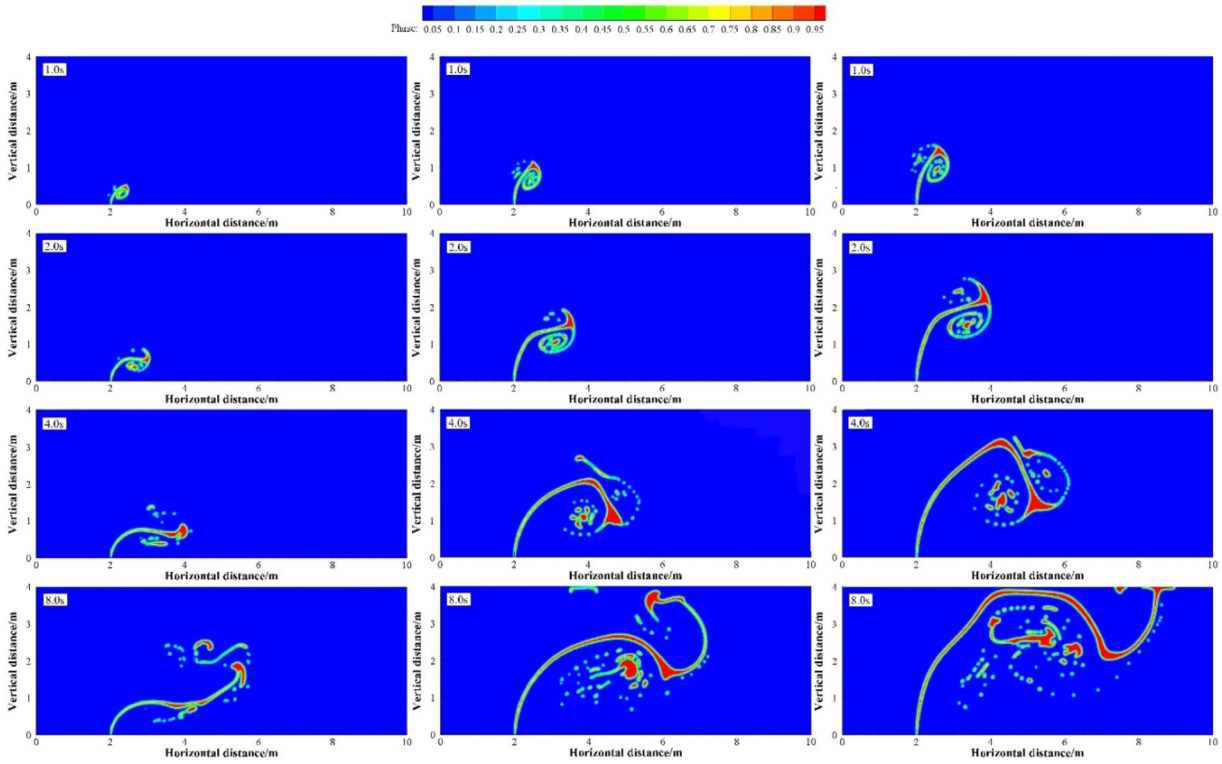

(a) Case 4 (b) Case 5 (c) Case 6

Figure 7. The migration and diffusion of underwater oil at different oil leaking rates when $U_w = 0.2\,m{\cdot}s^{-1}$.

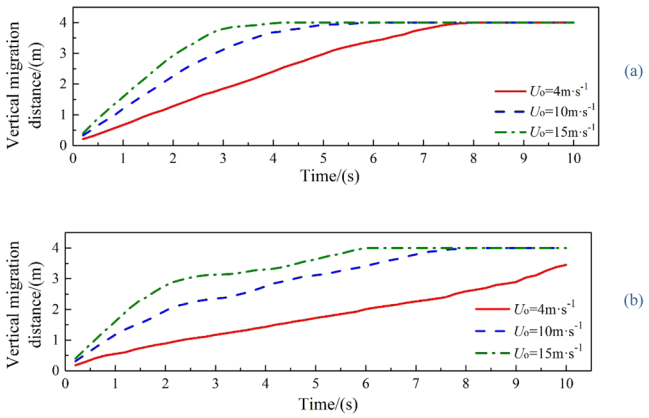

Figure 8. The vertical migration distance at different oil leaking rates when $U_w = 0.1\,m{\cdot}s^{-1}$ (**a**) and $U_w = 0.2\,m{\cdot}s^{-1}$ (**b**).

U_w is, the later the second stage appears. When ocean current velocity is large enough, the influence of ocean current is obviously dominant. The oil droplets that have just overflowed are washed away by ocean current[47], and the second entrainment motion does not occur any more (Figs. 11(c) and 12(c)). It can be seen from Fig. 13 that both U_{w1} and U_{o1} of the jet are negatively correlated with U_w.

Combined action of oil leaking rate (U_o) and ocean current velocity (U_w). Numerical simulation were carried out under four groups of simulation cases (Case 12 and 13; Case 4, 7 and 14; Case 15 to 17; Case 1, 18 and 19 as four groups, respectively). These four groups of cases were selected to discuss the effect of different R on underwater oil spill. The floating processes of oil spilling from the leak under different R are shown in Figs. 14–17.

It can be seen from the above that the increase of U_o and U_w respectively can both intensify the accumulation of oil droplets at the lower right side of the jet. The accumulation of oil under the water has a certain correlation

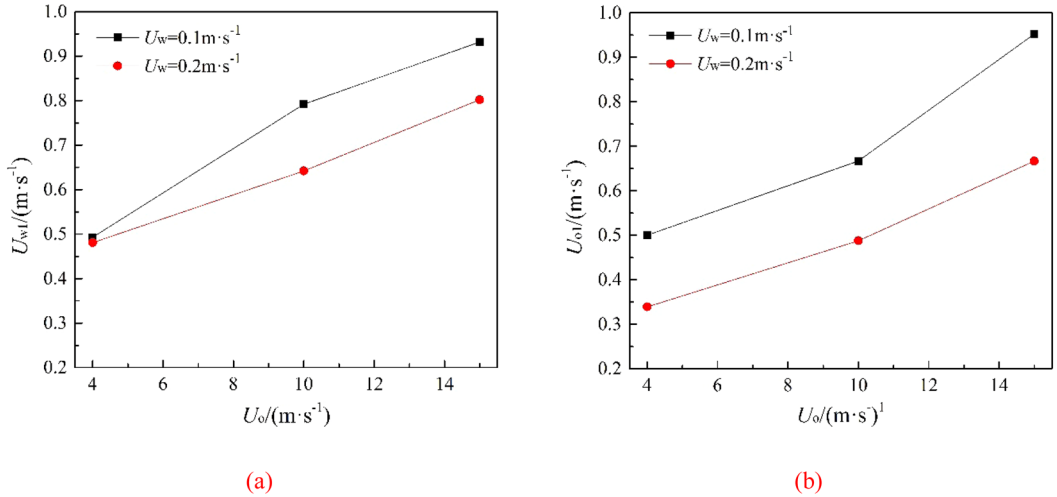

Figure 9. The average migration velocities of horizontal direction (**a**) and vertical direction (**b**) at different oil leaking rates when $U_w = 0.1\ m{\cdot}s^{-1}$ and $U_w = 0.2\ m{\cdot}s^{-1}$, respectively.

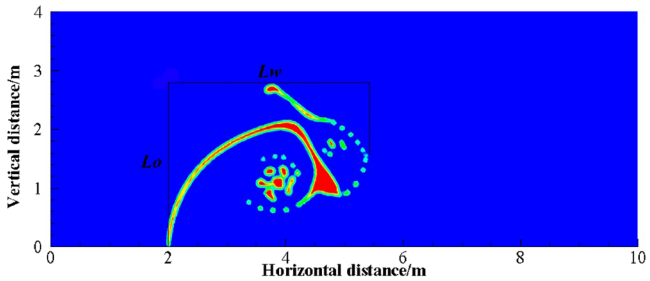

Figure 10. Definition of parameters of oil spill migration.

with U_o and U_w. We define that the ratio of U_o to U_w as R, and the ratio of U_{o1} to U_{w1} as R_1.The smaller R is, the more dispersed oil droplets accumulate. However, according to Figs. 14–17, the same R cannot guarantee the migration trajectory of the spilled oil to be consistent. When R is the same, but both U_o and U_w increase, the migration pattern of the jet is still similar to the trajectory migration pattern when only U_w increases. However, when R is small enough, even if the oil leaking rate is large enough, the spilled oil rushes directly to the right of the leak hole by the ocean current at the first stage[47] (Fig. 14). The larger U_o is, the longer the jet is affected by the initial momentum, and the later the second stage of free diffusion occurs. It can be known that, by the comparison of the two factors, the influence of U_w on the migration pattern of the oil spilling is greater than that of U_o on the jet. It can be seen that U_w is a more important reference than U_o to determine the migration and diffusion pattern and behavior of the spilled oil.

It can be seen from Fig. 18 that the values of U_{o1} and U_{w1} are basically the same when R is the same, and they are positively correlated with R, fluctuating within a small range. The value of R in this study was ranged from 5 to 150. We can obtain from Fig. 19 that R_1 ($R_1 = U_{o1}/U_{w1}$) is linearly positively correlated with R, but R_1 fluctuates within a small range (0.24 to 1.02). When $20 \leq R \leq 150$, R_1 increases uniformly in the range of 0.75 to 1.02, and it fits a linear fit curve (as shown in Fig. 20), and the adjust R-square is 0.92041. The fitting formula is as follow:

$$R_1 = 0.66932 + 0.00215R \tag{11}$$

However, under the extreme conditions of $R < 10$, this rule is not fully applicable. When R is small enough, the influence of the ocean current is obviously dominant, and the initial momentum is intercepted at the first stage. The spilled oil is washed away as soon as it overflows, and only when the initial momentum disappears at the second stage can it gradually migrate towards the surface.

Conclusions

The migration and diffusion of underwater oil spills were simulated, and the effects of different U_o, different U_w and the combined action of U_o and U_w on underwater oil spills were discussed. The main conclusions obtained are as follows:

(1) When U_w is constant, U_{o1} and U_{w1} are linearly positively correlated with U_o. The larger U_o is, the higher the initial momentum of the oil jet is, the less influential the ocean current poses on it, the wider the

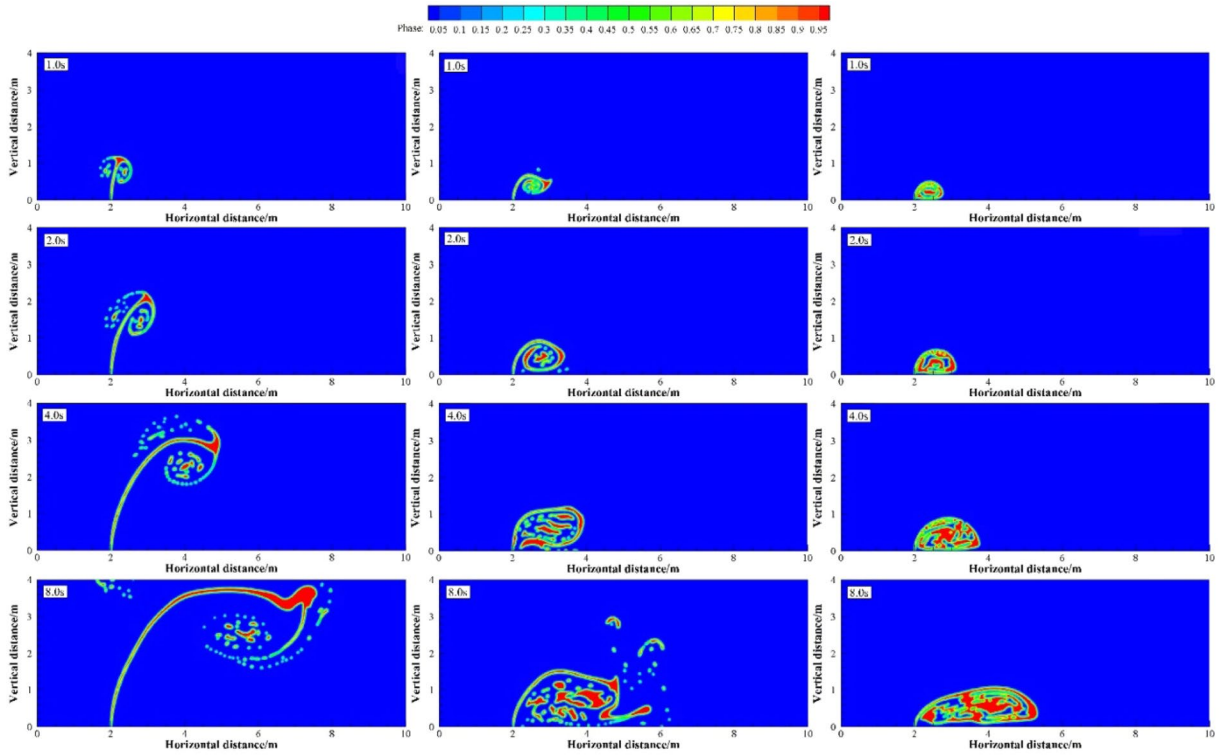

(a) Case 2 (b) Case 7 (c) Case 8

Figure 11. The migration and diffusion of underwater oil at different current velocities when $U_o = 10\,m{\cdot}s^{-1}$.

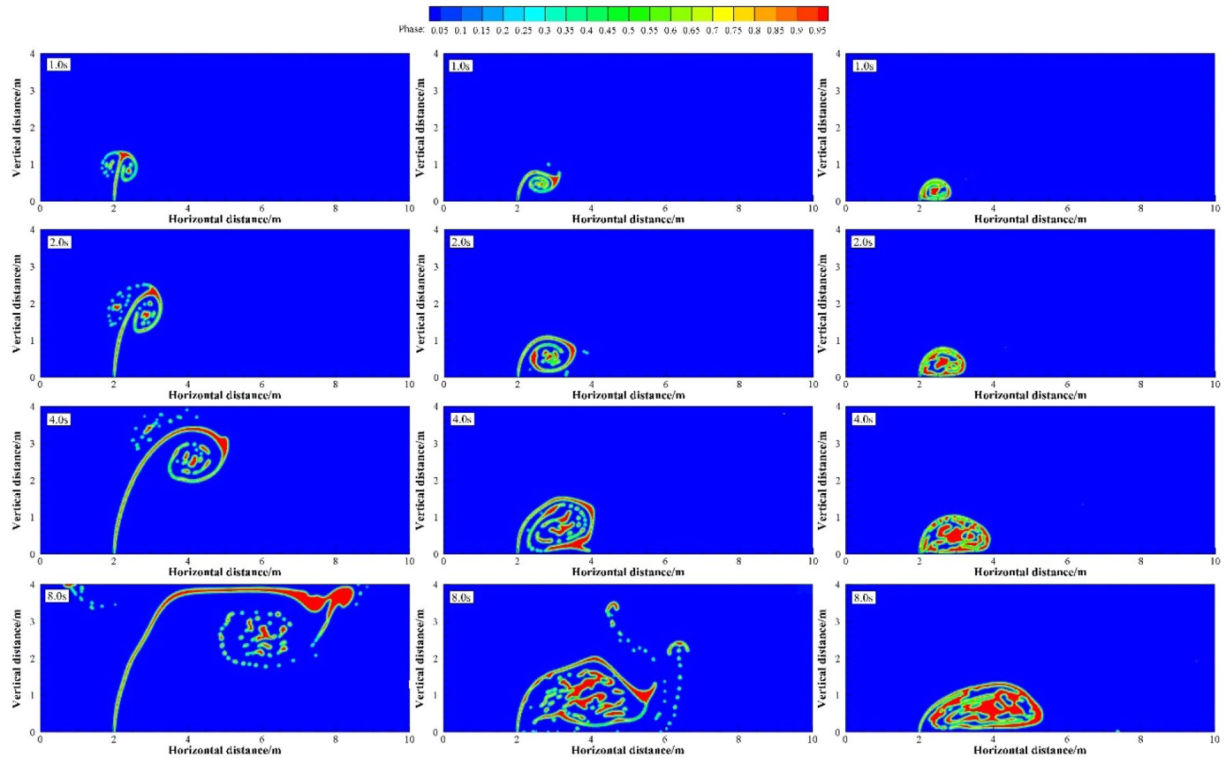

(a) Case 9 (b) Case 10 (c) Case 11

Figure 12. The migration and diffusion of underwater oil at different current velocities when $U_o = 12\,m{\cdot}s^{-1}$.

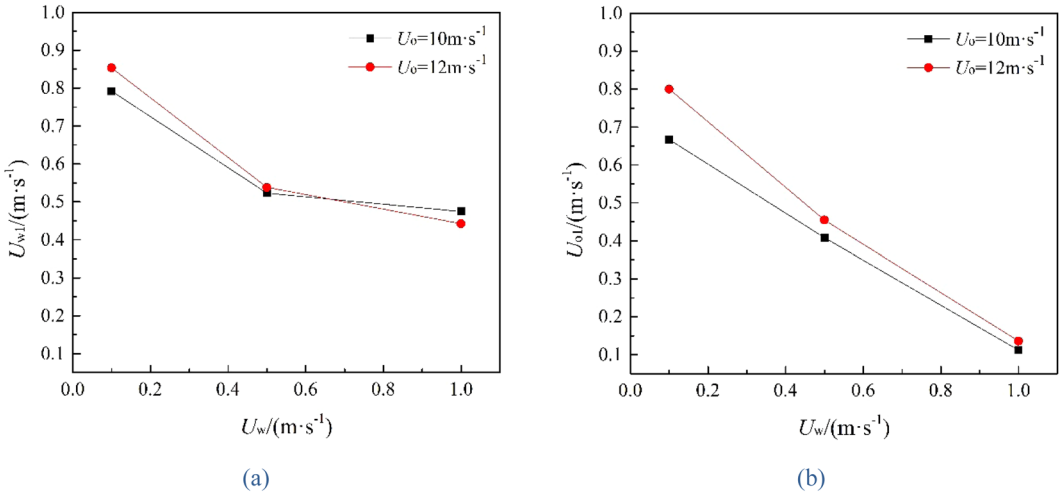

Figure 13. The average migration velocities of horizontal direction (**a**) and vertical direction (**b**) at different current velocities when $U_0 = 10\,\mathrm{m{\cdot}s^{-1}}$ and $U_0 = 12\,\mathrm{m{\cdot}s^{-1}}$, respectively.

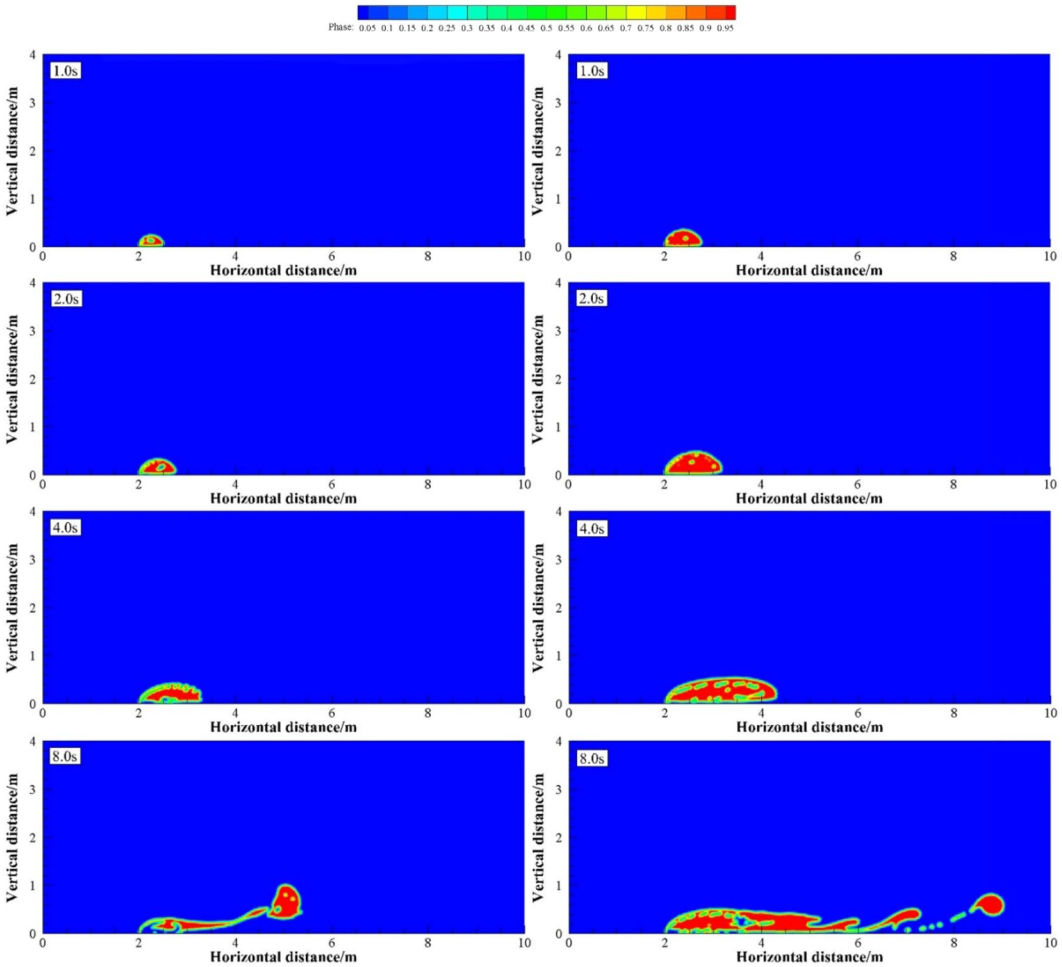

(a) Case 12 (b) Case 13

Figure 14. The migration and diffusion of underwater oil at different cases when $R = 5$.

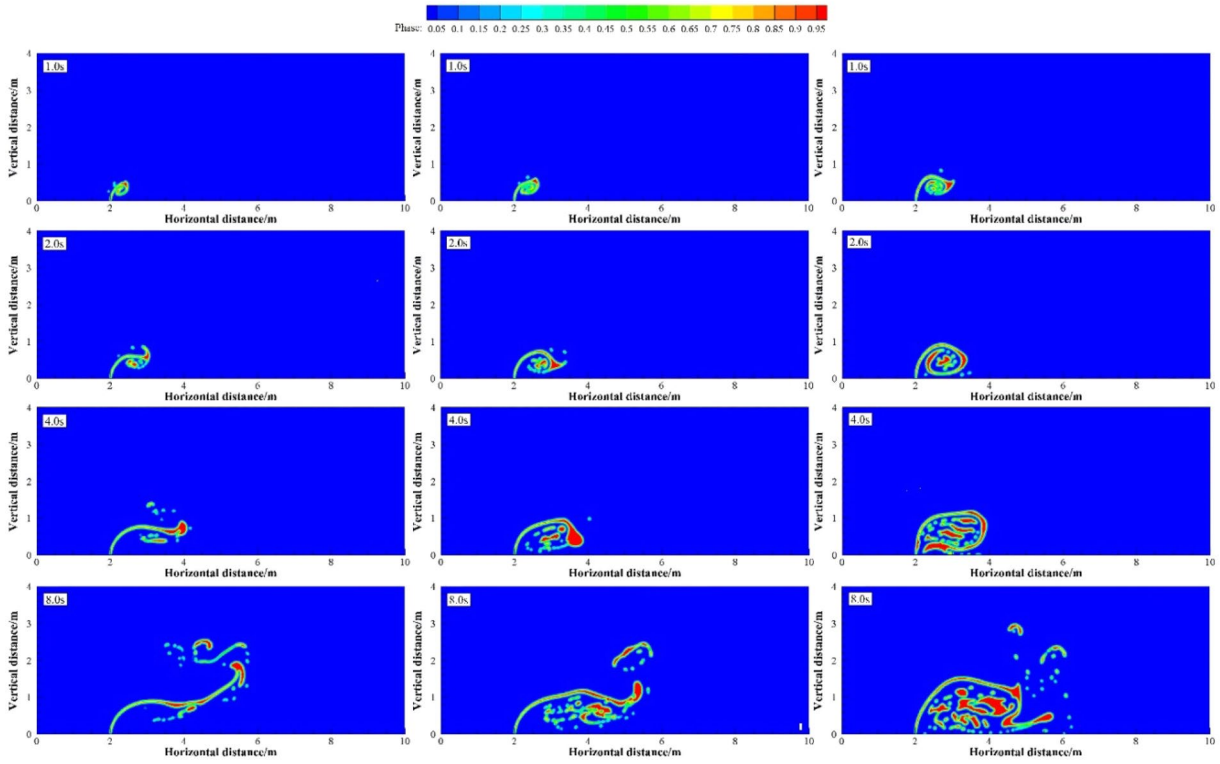

(a) Case 4 (b) Case 14 (c) Case 7

Figure 15. The migration and diffusion of underwater oil at different cases when $R = 20$.

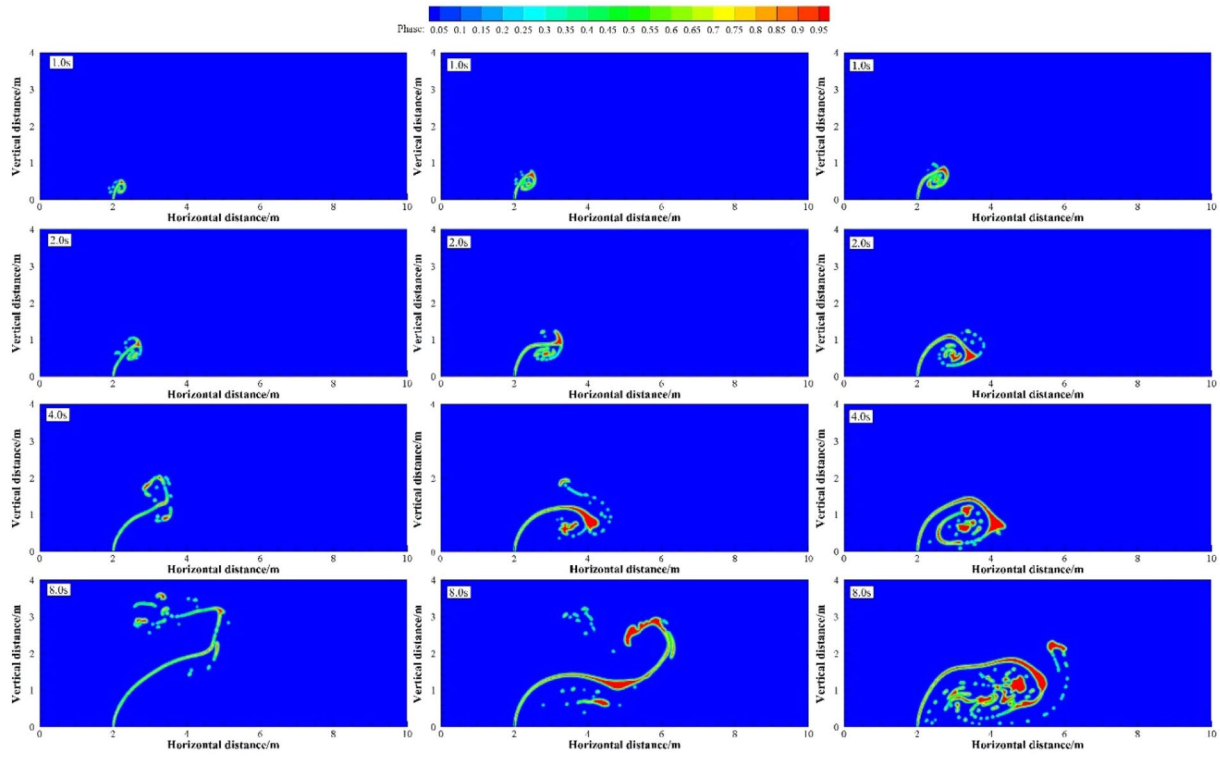

(a) Case 15 (b) Case 16 (c) Case 17

Figure 16. The migration and diffusion of underwater oil at different cases when $R = 30$.

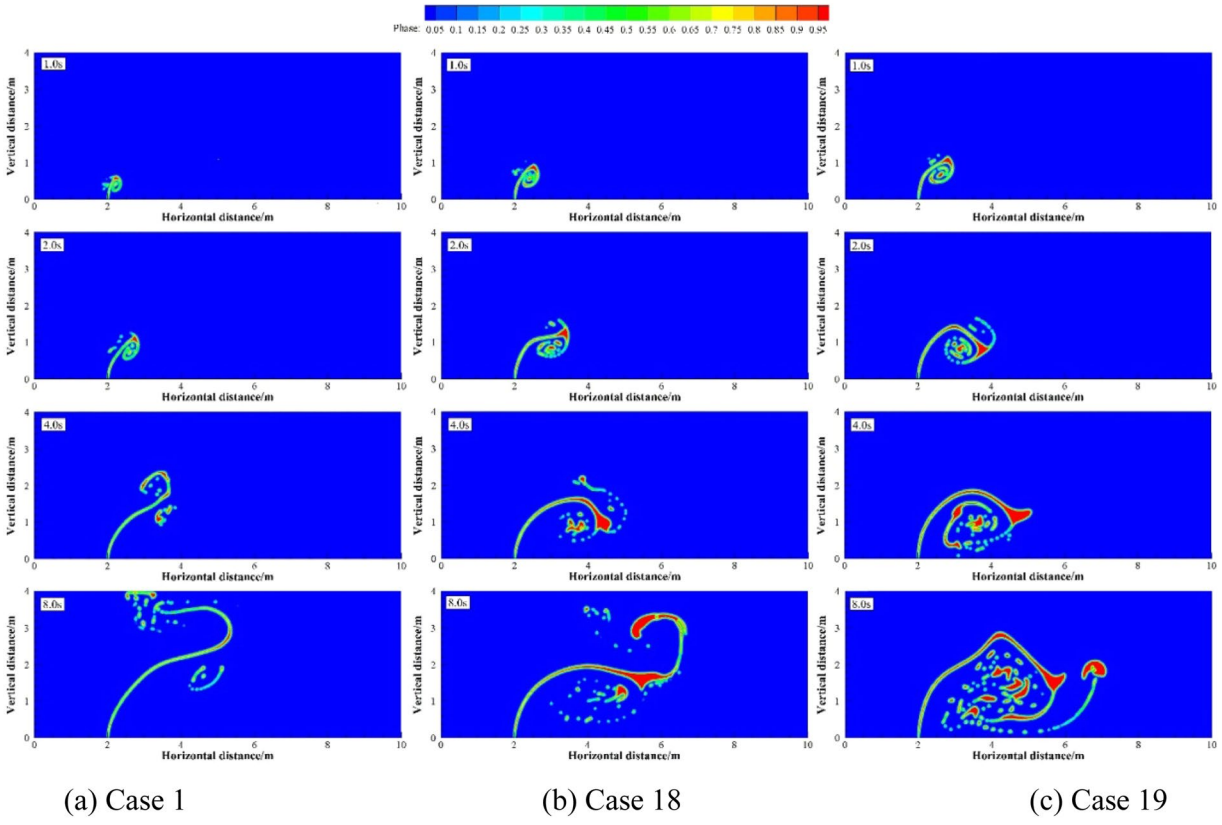

Figure 17. The migration and diffusion of underwater oil at different cases when $R = 40$.

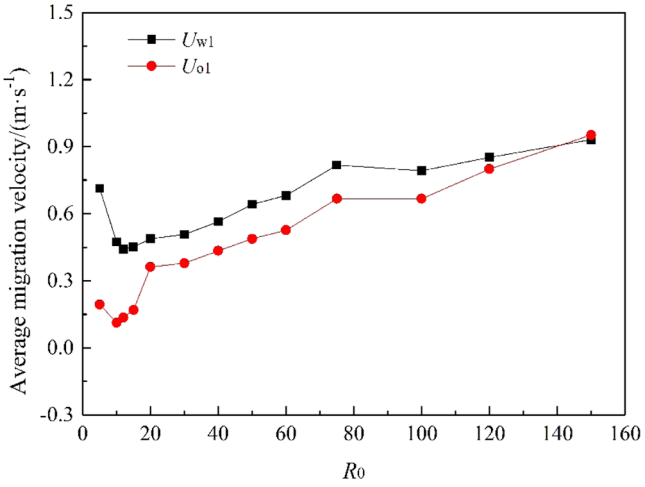

Figure 18. Average migration velocities at different R.

entrainment range is, and the more oil droplets accumulate in the vortex under the control of the entrainment movement and initial momentum. When U_o is constant, the larger U_w is, the larger the difference in the size of the first entrainment vortex on both sides of the jet is, the larger number and the lower height of oil droplets accumulate, and the more slowly the spilled oil migrates to the surface. The influence of ocean current is obviously dominant when U_w is large enough. Comparing the two factors, it can be obviously seen that the influence of U_w on the migration pattern of the oil spilling is greater than that of U_o.

(2) The smaller R is, the more dispersed oil droplets accumulate together. And when R is small enough, the initial momentum is controlled by the ocean current. It can only gradually float to the surface of the water under the motion of its own buoyancy and current after the initial momentum disappears.

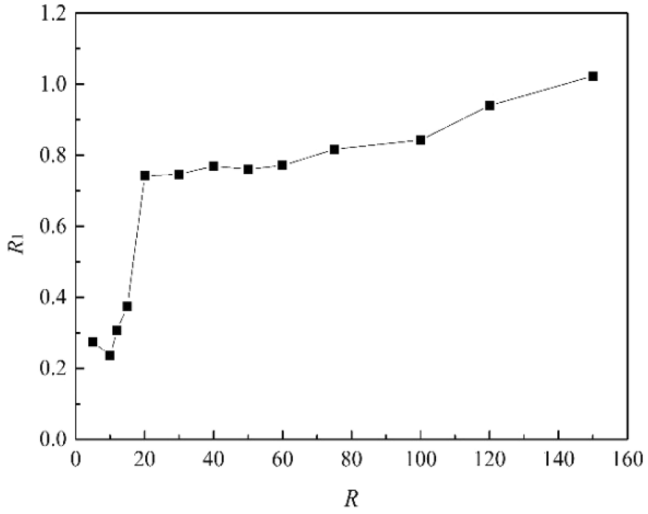

Figure 19. R_1 (Ratio of U_{o1} and U_{w1}) at different R.

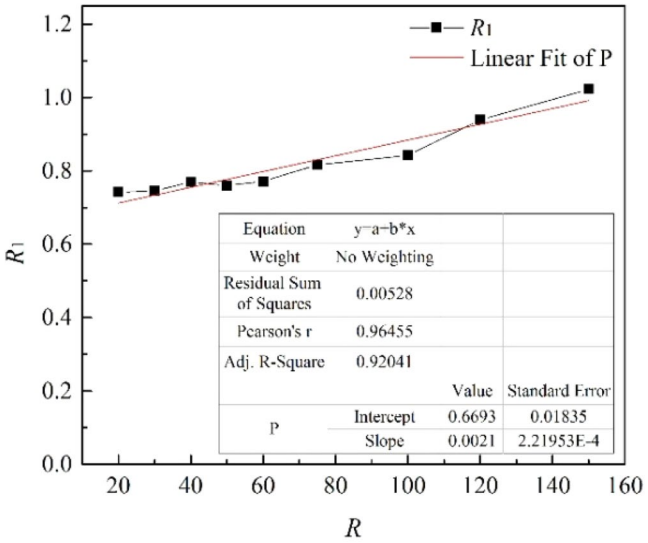

Figure 20. R_1 fitted curve with R values from 20 to 150.

(3) The average migration velocities are positively correlated with R, fluctuating within a small range of 0 to 1.1 $m \cdot s^{-1}$. R_1 ($R_1 = U_{o1}/U_{w1}$) is linearly positively correlated with R, fluctuating within a small range of 0.2 to 1.1, no matter how large R is. The linear fit curve is that $R_1 = 0.66932 + 0.00215R$.

Received: 7 March 2020; Accepted: 12 May 2020;
Published online: 08 June 2020

References

1. Alves, T. M. *et al*. Multidisciplinary oil spill modeling to protect coastal communities and the environment of the Eastern Mediterranean Sea. *Scientific Reports* **6**, 36882, https://doi.org/10.1038/srep36882 (2016).
2. Ding, L. P. *et al*. Plant-Inspired Layer-by-Layer Self-Assembly of Super-Hydrophobic Coating for Oil Spill Cleanup. *Polymers* **11**, https://doi.org/10.3390/polym11122047 (2019).
3. Li, Z. G., Jiang, M. R. & Yu, J. X. Numerical simulation on the oil spill for the submarine pipeline based on VOF method. *The Ocean Engineering* **34**, 100–110 (2016).
4. Yapa, P. D. & Li, Z. Simulation of oil spills from underwater accidents I: Model development. *Journal of Hydraulic Research* **35**, 673–688, https://doi.org/10.1080/00221689709498401 (1997).
5. Wang, S. D. *Study on the forecast models for oil spills in seas based on lagrange tracking* doctor thesis, Dalian University of Technology, (2008).
6. Hirst, E. Buoyant jets with three-dimensional trajectories. *Journal of Hydraulics Division* **98**, 1999–2014 (1972).
7. McDougall, T. J. Bubble plumes in stratified environments. *Journal of Fluid Mechanics* **85**, 655–672 (1978).

8. Milgram, J. H. Mean flow in round bubble plumes. *Journal of Fluid Mechanics* **133**, 345–376, https://doi.org/10.1017/S0022112083001950 (1983).
9. Fannelop, T. K., Hirschberg, S. & Küffer, J. Surface current and recirculating cells generated by bubble curtains and jets. *Journal of Fluid Mechanics* **229**, 629–657, https://doi.org/10.1017/S0022112091003208 (1991).
10. Bemporad, G. A. Simulation of Round Buoyant Jet in Stratified Flowing Environment. *Journal of Hydraulic Engineering* **120**, 529–543, doi:10.1061/(ASCE)0733-9429(1994)120:5(529) (1994).
11. Johansen, Ø. Development and verification of deep-water blowout models. *Marine Pollution Bulletin* **47**, 360–368, https://doi.org/10.1016/S0025-326X(03)00202-9 (2003).
12. Zheng, L. & Yapa, P. D. Simulation of oil spills from underwater accidents II: Model verification. *Journal of Hydraulic Research* **36**, 117–134, https://doi.org/10.1080/00221689809498381 (1998).
13. Dasanayaka, L. K. & Yapa, P. D. Role of plume dynamics phase in a deepwater oil and gas release model. *Journal of Hydro-environment Research* **2**, 243–253, https://doi.org/10.1016/j.jher.2009.01.004 (2009).
14. North, E. W. *et al*. Simulating Oil Droplet Dispersal From the Deepwater Horizon Spill With a Lagrangian Approach. *Washington DC American Geophysical Union Geophysical Monograph Series* **195**, 217–226, https://doi.org/10.1029/2011GM001102 (2011).
15. Yapa, P. D., Wimalaratne, M. R., Dissanayake, A. L. & DeGraff, J. A. Jr. How does oil and gas behave when released in deepwater? *Journal of Hydro-environment Research* **6**, 275–285, https://doi.org/10.1016/j.jher.2012.05.002 (2012).
16. Ben-Mansour, R., Habib, M. A., Khalifa, A., Youcef-Toumi, K. & Chatzigeorgiou, D. Computational fluid dynamic simulation of small leaks in water pipelines for direct leak pressure transduction. *Computers & Fluids* **57**, 110–123, https://doi.org/10.1016/j.compfluid.2011.12.016 (2012).
17. Reed, M. *et al*. Numerical model for estimation of pipeline oil spill volumes. *Environmental Modelling & Software* **21**, 178–189, https://doi.org/10.1016/j.envsoft.2004.04.019 (2006).
18. Liao, G. X., Gao, Z. H. & Xiong, D. Q. A model for simulating the transport and diffusion of oil and gas released in underwater spill accidents. *Journal of Dalian Maritime University* **36**, 115–120 (2010).
19. Chen, H. B. *et al*. Numerical simulation of underwater oil spill. *The Ocean Engineering* **33**, 66–76 (2015).
20. Lu, S. C., Zhang, J., Wu, S. J. & Pang, C. Experiments and numerical simulation on the horizontal leakage of submarine pipelines. *Oil & Gas Storage and Transportation* **37**, 469–474 (2018).
21. Li, X. H., Li, X. M., Chen, G. M. & Zhu, H. W. Study on the dispersion characteristics of leaking oil and gas from subsea separator in 2000 m ultra deepwater. *Journal of Safety Science and Technology* **12**, 38–43 (2016).
22. Li, Y. Q. *Drift forecasting model and risk assessment of Bohai sunken and submerged oil* Master of engineering thesis, Dalian Marritime University, (2015).
23. Lu, S. C., Zhang, J., Zang, X. G., Gong, X. & Chen, H. M. Analysis on the sensitivity of submarine pipeline leakage parameters. *Journal of Ocean Technology* **35**, 103–107 (2016).
24. Zhu, H. J., You, J. H. & Zhao, H. L. Underwater spreading and surface drifting of oil spilled from a submarine pipeline under the combined action of wave and current. *Applied Ocean Research* **64**, 217–235 (2017).
25. Zhu, H. J., You, J. H. & Zhao, H. L. An experimental investigation of underwater spread of oil spill in a shear flow. *Marine Pollution Bulletin* **116**, 156–166, https://doi.org/10.1016/j.marpolbul.2017.01.002 (2017).
26. Zhu, H. J., Lin, P. Z. & Pan, Q. A CFD (computational fluid dynamic) simulation for oil leakage from damaged submarine pipeline. *Energy* **64**, 887–899, https://doi.org/10.1016/j.energy.2013.10.037 (2014).
27. Yang, Z. L. *et al*. Application of computational fluid dynamics simulation for submarine oil spill. *Acta Oceanologica Sinica* **37**, 104–115 (2018).
28. Mossa, M. & Davies, P. Some Aspects of Turbulent Mixing of Jets in the Marine Environment. *Water* **10** (2018).
29. Meftah, M. B. & Mossa, M. Turbulence Measurement of Vertical Dense Jets in Crossflow. *Water* **10**.
30. De Padova, D., Mossa, M. & Sibilla, S. Characteristics of nonbuoyant jets in a wave environment investigated numerically by SPH. *Environmental Fluid Mechanics* **20**, 189–202, https://doi.org/10.1007/s10652-019-09712-x (2020).
31. Barile, S., De Padova, D., Mossa, M. & Sibilla, S. Theoretical analysis and numerical simulations of turbulent jets in a wave environment. *Physics of Fluids* **32**, 035105, https://doi.org/10.1063/1.5141039 (2020).
32. Leifer, I. *et al*. Satellite and airborne oil spill remote sensing: State of the art and application to the BP DeepWater Horizon oil spill. *Proceedings of the 34th AMOP Technical Seminar on Environmental Contamination and Response*, 270–295 (2011).
33. De Carolis, G., Adamo, M., Pasquariello, G., De Padova, D. & Mossa, M. Quantitative characterization of marine oil slick by satellite near-infrared imagery and oil drift modelling: The Fun Shai Hai case study. *International Journal of Remote Sensing* **35**, 1838–1854, https://doi.org/10.1080/01431161.2012.727494 (2013).
34. De Padova, D., Mossa, M., Adamo, M., De Carolis, G. & Pasquariello, G. Synergistic use of an oil drift model and remote sensing observations for oil spill monitoring. *Environmental Science and Pollution Research* **24**, https://doi.org/10.1007/s11356-016-8214-8 (2017).
35. Van Maele, K. & Merci, B. Application of two buoyancy-modified k–ε turbulence models to different types of buoyant plumes. *Fire Safety Journal* **41**, 122–138, https://doi.org/10.1016/j.firesaf.2005.11.003 (2006).
36. P., R. & B., M. Numerical predictions of indoor climate in large industrial premises. A comparison between different k-ε models supported by field measurements. *Building and Environment* **42**, 3872–3882 (2007).
37. Fay, J. A. & Hoult, D. P. Physical processes in the spread of oil on a water surface. *International Oil Spill Conference Proceedings* **1971**, 463–467 (1971).
38. Hieu, P. D., Katsutoshi, T. & Ca, V. T. Numerical simulation of breaking waves using a two-phase flow model. *Applied Mathematical Modelling* **28**, 983–1005, https://doi.org/10.1016/j.apm.2004.03.003 (2004).
39. Hirt, C. W. & Nichols, B. D. Volume of fluid (VOF) method for the dynamics of free boundaries. *Journal of Computational Physics* **39**, 201–225, https://doi.org/10.1016/0021-9991(81)90145-5 (1981).
40. Lin, M. H., He, G. X., Li, Y. S., Tang, D. D. & Liang, Y. T. A numerical simulation on the spilled oil diffusion of submarine pipelines. *Journal of Bejing Institute of Petrochemical Technology* **25**, 83–90 (2017).
41. Lv, G. L., Zhang, J., Yang, Y. P. & Liu, Z. M. Simulation and analysis of duffusion of oil and gas leakage from submarine pipelines based on CFD. *Journal of Jimei University (Natural Science)* **22**, 51–57 (2017).
42. Xie, N., Luo, X. K., Xue, W. D., Liang, Y. T. & He, G. X. Numerical simulation analysis of the diffusion of refined oil in water. *Petroleum Planning & Engineering* **27**, 9–12 (2015).
43. Zhang, J., Zang, X. G., Zhang, Y. C., He, H. Z. & Chen, H. M. Dynamic characteristics of plume/jet from underwater pipe downward leakage. *Journal of Chemical Industry and Engineering (China)* **67**, 4969–4975 (2016).
44. Qi, J. L. *et al*. Study on underwater oil spill behavior and fate in deep water area. *Ocean Development and Management* **30**, 77–84 (2013).
45. Wang, Q., Shi, W., Yu, X. & Zhou, X. T. Influence of different water flow speed on the oil spill of submarine pipeline. *Contemporary Chemical Industry* **47**, 1460–1463 (2018).
46. Zang, X. G. Study on characteristics of pipeline leakage and oil-gas diffusion, *Jimei University*, (2016).
47. Wang, W. Q., Li, Z. Y., Ma, G. Y., Liu, L. & Wang, H. L. Numerical study on crude oil leakage of underwater pipeline. Energy Conservation. *Technology* **29**, 311–314 (2011).

Acknowledgements
The authors also thank Deqi Wang, Gao Zhang and Weikang Liu for providing helps in the course of the experiments. This research was funded by the National Natural Science Foundation of China (No. 51704041 and No. 51574044), the Nature Science Foundation of Jiangsu Province (No. BK20150269), the Major Research Plan of the Oil and Gas Storage and Transportation Laboratory of Jiangsu Province (No. SCZ1211200004/004), the Changzhou University Fund Project (No. ZMF14020055), and the Postgraduate Research & Practice Innovation Program of Jiangsu Province (No. KYCX18_2630).

Author contributions
Conceptualization, H.J.; methodology, H.J. and M.X.; software, H.J. and M.X.; validation, H.J. and M.X.; formal analysis, H.J. and M.X.; investigation, H.J. and M.X.; resources, H.J., K.Y. and W.H.; data curation, H.J. and M.X.; writing—original draft preparation, H.J. and M.X.; writing—review and editing, H.J.; visualization, H.J. and M.X.; supervision, H.J.; project administration, H.J.; funding acquisition, H.J., M.X., K.Y. and W.H.; All authors have read and agreed to the published version of the manuscript.

Competing interests
The authors declare no competing interests.

Additional information
Correspondence and requests for materials should be addressed to W.H. or K.Y.

Reprints and permissions information is available at www.nature.com/reprints.

Publisher's note Springer Nature remains neutral with regard to jurisdictional claims in published maps and institutional affiliations.